DALTON

Carbon-13 nuclear magnetic resonance of transition-metal carbonyl clusters through intermolecular cross-polarisation transfer in the solid state

Taro Eguchi,*[a] Rachel A. Harding,[a,b] Brian T. Heaton,*[b] Giuliano Longoni,[c] Kei Miyagi,[a] Jens Nähring,[b] Nobuo Nakamura,[a] Hirokazu Nakayama[a] and Anthony K. Smith[b]

[a] *Department of Chemistry, Graduate School of Science, Osaka University, Toyonaka, Osaka 560 Japan*
[b] *Department of Chemistry, University of Liverpool, Liverpool L69 3BX, UK*
[c] *Dipartimento di Chimica Fisica ed Inorganica, Viale del Risorgimento 4, 40136, Bologna, Italy*

The ^{13}C cross polarisation magic angle spinning NMR spectra of $[Ni_6(CO)_{12}]^{2-}$ at natural ^{13}C abundance have been recorded with four different cations, $[NMe_4]^+$, $[NEt_4]^+$, $[AsPh_4]^+$ and $[N(PPh_3)_2]^+$ and the crystal structure of the previously unreported $[AsPh_4]^+$ salt of $[Ni_6(CO)_{12}]^{2-}$ has been determined. Carbonyl resonances of the anion at natural ^{13}CO abundance with excellent signal-to-noise ratio (*ca.* 1:1 for a single scan) are only observed for $[NMe_4]_2[Ni_6(CO)_{12}]$ and the possible reasons for this are discussed.

In the course of our continuing work to understand the dynamic behaviour of transition-metal carbonyl clusters in the solid state,[1–3] ^{13}CO resonances with good signal-to-noise ratio (*ca.* 0.14:1 for a single scan) have been observed for $[NMe_4]_2[Ni_{12}(CO)_{21}H_2]$ at natural ^{13}CO abundance.[4] It is very surprising to observe ^{13}CO signals for transition-metal carbonyl clusters with such good signal-to-noise ratio without ^{13}CO enrichment. In order to investigate this further, ^{13}C cross polarisation magic angle spinning (CP MAS) spectra of a series of $[Ni_6(CO)_{12}]^{2-}$ clusters have now been recorded for four different cations, $[NMe_4]^+$, $[NEt_4]^+$, $[AsPh_4]^+$ and $[N(PPh_3)_2]^+$. The values of the proton relaxation times T_1 and $T_{1\rho}$ have been measured to determine the origin of the cross polarisation and line broadening due to molecular motion. The crystal structures of the $[NMe_4]^+$ and $[N(PPh_3)_2]^+$ salts have been reported previously[5,6] and, in order to compare interatomic H···CO distances, we now report the structure of the $[AsPh_4]^+$ salt of $[Ni_6(CO)_{12}]^{2-}$. The structure of the anion in all these salts is similar and consists of a distorted Ni_6 trigonal antiprism with one terminal CO on each Ni and each of the six triangular nickel edges is bridged by one CO. Crystallographic data for all of these salts are summarised in Table 1. Unfortunately, it was not possible to obtain X-ray-quality crystals of $[NEt_4]_2[Ni_6(CO)_{12}]$.

Consistent with the solid-state structure, there are two equally intense ^{13}CO NMR resonances in solution at δ *ca.* 237 and 197 due to bridge and terminal CO, respectively.[7]

The crystallographic data show that the site symmetry of $[Ni_6(CO)_{12}]^{2-}$ is S_6 for the $[NMe_4]^+$ salt and C_i for both the $[AsPh_4]^+$ and $[N(PPh_3)_2]^+$ salts. Thus, for the $[NMe_4]^+$ salt there should be only one ^{13}CO resonance in the solid state for each of the terminal and bridging CO whereas there could be up to three resonances for each of the terminal and bridging CO for the other two salts.

Results and Discussion

The ^{13}CO CP MAS NMR spectra of $[Ni_6(CO)_{12}]^{2-}$ at the natural ^{13}C abundance level are shown in Figs. 1–3 for four different cations, $[NMe_4]^+$, $[NEt_4]^+$, $[AsPh_4]^+$ and $[N(PPh_3)_2]^+$. For the $[NMe_4]^+$ salt two intense, sharp ^{13}CO resonances are detected at δ 239.0 and 200.6; they can be observed quickly (480 scans) and have chemical shifts similar to those found in solution for the bridging and terminal carbonyls respectively [Fig. 2(*a*)]. For the

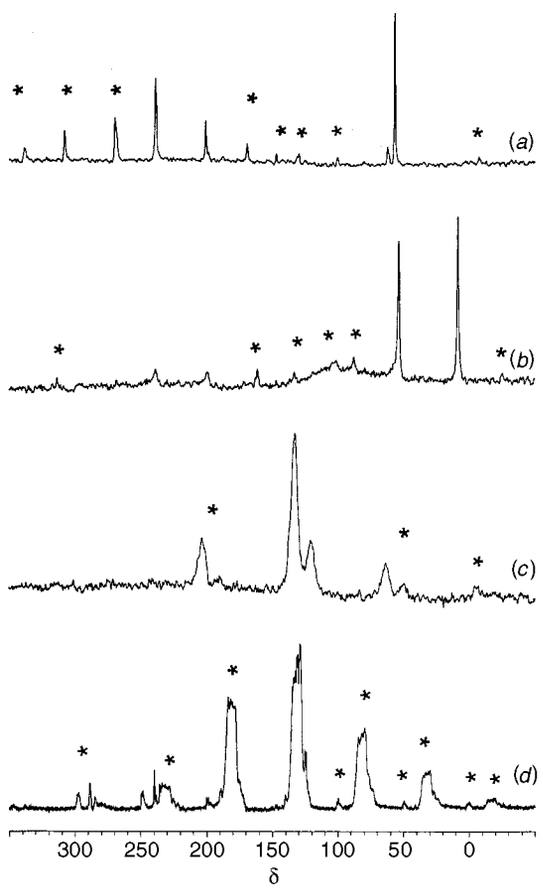

Fig. 1 The ^{13}C CP MAS NMR spectra of (*a*) $[NMe_4]_2[Ni_6(CO)_{12}]$ (480 scans) with MAS rate = 3.5 kHz, (*b*) $[NEt_4]_2[Ni_6(CO)_{12}]$ (6640 scans) with MAS rate = 4.0 kHz, (*c*) $[AsPh_4]_2[Ni_6(CO)_{12}]$ (2400 scans) with MAS rate = 3.5 kHz, and (*d*) $[N(PPh_3)_2]_2[Ni_6(CO)_{12}]$ (13 000 scans) with MAS rate = 2.5 kHz, at room temperature; * represents the spinning side band

$[NEt_4]^+$ salt [Fig. 2(*b*)] the signal-to-noise ratio of the two ^{13}CO resonances at δ 238 and 198 is much worse despite much longer collection times (see legend for Fig. 1). In the case of the $[AsPh_4]^+$ salt [Fig. 2(*c*)] we were not able to detect the carbonyl

Table 1 Crystallographic data for $[Ni_6(CO)_{12}]^{2-}$ with different cations

	Cation		
	$[NMe_4]^+$ [5]	$[AsPh_4]^+$	$[N(PPh_3)_2]^+$ [6]
Crystal form	Trigonal	Triclinic	Triclinic
Space group	$P\bar{3}$	$P\bar{1}$	$P\bar{1}$
a/Å	11.003(1)	11.760(5)	13.299(4)
b/Å	11.003(1)	12.648(5)	13.343(4)
c/Å	7.045(1)	11.266(6)	13.051(5)
α/°	90.00(0)	103.15(4)	106.24(3)
β/°	90.00(0)	117.42(3)	119.04(2)
γ/°	120.00(0)	95.72(4)	81.41(3)
U/Å^3	738.7	1407(1)	1943(1)
D_c/g cm^{-3}	1.88	1.717	1.508
Z	1	1	1
T[a]/K	298	153	296
d(Ni–Ni)[b]	2.38	2.379(2)	2.392(5)
d(Ni–Ni)[c]	2.77	2.745(5)	2.789(4)
		2.847(3)	2.761(5)

[a] Temperature used to collect X-ray data. [b] Within the $Ni_3(CO)_3(\mu\text{-}CO)_3$ plane. [c] Between the $Ni_3(CO)_3(\mu\text{-}CO)_3$ planes.

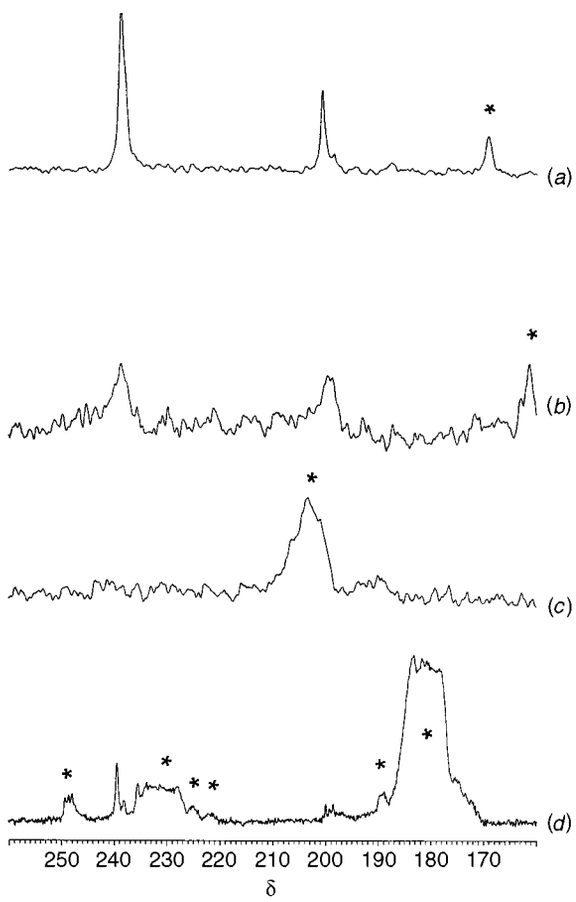

Fig. 2 Expanded plots of Fig. 1 in the carbonyl resonance region

resonances, even on changing the spinning rate from 2 to 4 kHz to eliminate the interference due to the spinning side bands. On the contrary, for the largest cation, $[N(PPh_3)_2]^+$ [Figs. 2(*d*) and 3], very weak but sharp bridging carbonyl resonances were found at δ 239.5, 238.0, and 235.4, and terminal resonances at δ 200.0, 199.3 and 198.5, respectively; the occurrence of three resonances in each of the bridging and terminal regions is consistent with the site symmetry of the anion as described above.

These and other presently unpublished results [4] show that the signal-to-noise ratio of ^{13}CO resonances in CP MAS measurements of anionic carbonyl clusters appear to be much higher when $[NMe_4]^+$ salts are used. We thus examine below some of

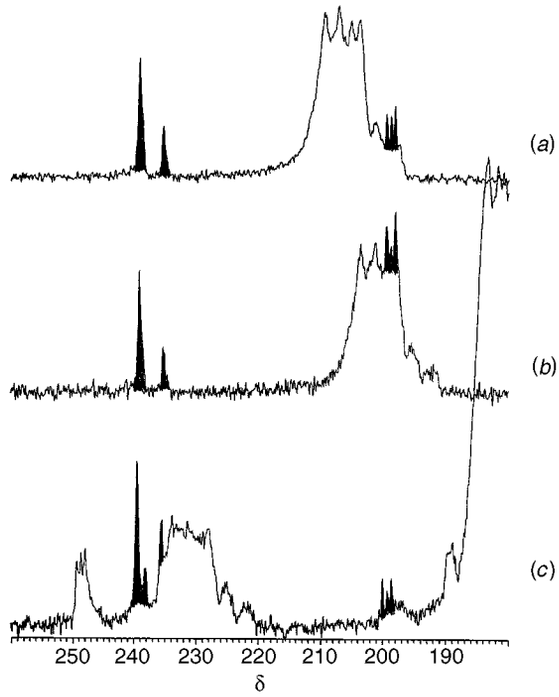

Fig. 3 Carbonyl resonance region in ^{13}C CP MAS NMR spectra of $[N(PPh_3)_2]_2[Ni_6(CO)_{12}]$ with MAS rate = (*a*) 3.8 (12 700), (*b*) 3.5 (2540), and (*c*) 2.5 kHz (13 000 scans). Shaded peaks represent the real carbonyl resonances. The linewidths of the bridging CO (near δ 240) become slightly broad on increasing the MAS rate

the factors which could be responsible for this enhancement. Many factors are known to influence the signal-to-noise ratio of ^{13}C resonances in CP MAS measurements.[8–12]

The structure of the anion $[Ni_6(CO)_{12}]^{2-}$ in the $[NMe_4]^+$,[5] $[AsPh_4]^+$ and $[N(PPh_3)_2]^+$ [6] salts is quite similar and consists of two planar $Ni_3(CO)_3(\mu\text{-}CO)_3$ groups in a trigonal-antiprismatic arrangement; for the $[NMe_4]^+$ salt all six values of d(Ni–Ni) between the two $Ni_3(CO)_3(\mu\text{-}CO)_3$ planes are similar whereas in the $[AsPh_4]^+$ and $[N(PPh_3)_2]^+$ salts the trigonal antiprism is slightly distorted resulting in two shorter and four longer Ni–Ni distances between these two planes (see Table 1) and this static distorted structure is retained on the NMR time-scale (see above). In all cases the value of d(Ni–Ni) is significantly shorter within the $Ni_3(CO)_3(\mu\text{-}CO)_3$ plane than between these planes.

The different packing arrangements induced on changing the cation {$[NMe_4]^+$, $[AsPh_4]^+$, $[N(PPh_3)_2]^+$} are represented schematically in Fig. 4(*a*)–4(*c*), respectively. These variations are difficult to predict and rationalise but it is of interest that for $[NMe_4]_2[Ni_6(CO)_{12}]$ the Ni_6 units stack with adjacent staggered $Ni_3(CO)_3(\mu\text{-}CO)_3$ planes [Fig. 4(*a*)] whereas phenyl rings from both $[AsPh_4]^+$ and $[N(PPh_3)_2]^+$ separate these $Ni_3(CO)_3(\mu\text{-}CO)_3$ planes between adjacent Ni_6 units [Fig. 4(*b*), 4(*c*)]. Fig. 4 also shows the minimum interatomic H···CO contacts for both terminal and bridging carbonyls. These distances, which are based on the calculated H atom positions, have been calculated using the ORFFE program [13] and are summarised in Table 2.

With increasing bulk of the cation the density of the $[Ni_6(CO)_{12}]^{2-}$ salts decreases and the calculated densities of the $[NMe_4]^+$, $[AsPh_4]^+$ and $[N(PPh_3)_2]^+$ salts are 1.88, 1.717 and 1.508 g cm^{-3} respectively but this can only have a minor effect on the variation of the signal-to-noise ratio for these different salts.

As outlined in the introduction, the anion site symmetry in the unit cell is S_6 for the $[NMe_4]^+$ and C_i for the $[AsPh_4]^+$ and $[N(PPh_3)_2]^+$ salts. If all other factors are equal then this could lead to a maximum signal-to-noise ratio reduction by a factor of 3 on changing the cation from $[NMe_4]^+$ to $[AsPh_4]^+$ or $[N(PPh_3)_2]^+$. It is, therefore, obvious that the anion site symmetry

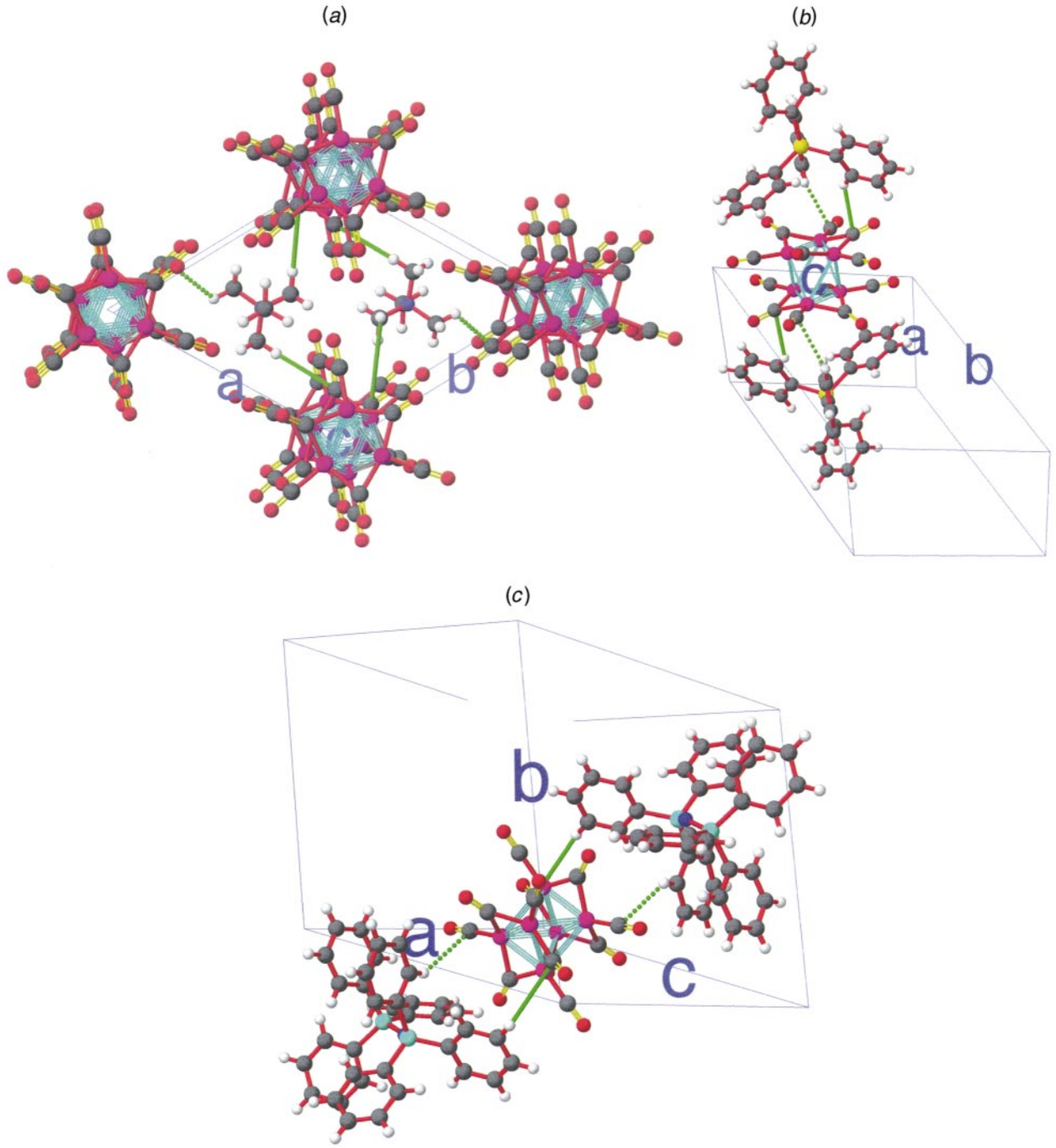

Fig. 4 Packing diagrams of different salts of $[Ni_6(CO)_{12}]^{2-}$: (*a*) $[NMe_4]^+$, (*b*) $[AsPh_4]^+$ and (*c*) $[N(PPh_3)_2]^+$. Hydrogen atoms white, carbon grey, oxygen red, nitrogen blue, arsenic yellow, phosphorus cyan, nickel magenta, green solid lines shortest $H\cdots CO_{bridge}$ and green dotted lines shortest $H\cdots CO_{terminal}$

plays an important role. However, the observed reduction is greater (see Fig. 2) and other factors must also be taken into account.

Even if the Hartmann–Hahn condition, $\gamma_C H_1^C = \gamma_H H_1^H$, is fulfilled in the cross-polarisation experiment, the signal intensity is determined by the kinetics of magnetisation transfer. It depends on the contact time or cross-polarisation time t_m according to equations (1) and (2).[8–10] These equations show

$$M(t_m) = M_0\lambda^{-1}\left[1 - \exp\left(-\frac{\lambda t_m}{T_{CH}}\right)\right]\exp\left[-\frac{t_m}{T_{1\rho}(^1H)}\right] \quad (1)$$

$$\lambda = 1 + \frac{T_{CH}}{T_{1\rho}(^{13}C)} - \frac{T_{CH}}{T_{1\rho}(^1H)} \quad (2)$$

that the magnetisation M increases with a time constant $\lambda^{-1}T_{CH}$ during the short contact time t_m of the ^{13}C nuclei with the ^1H nuclei, if the cross-relaxation time, T_{CH}, is sufficiently short compared with $T_{1\rho}(^{13}C)$ and $T_{1\rho}(^1H)$. Subsequently, a reduction in the magnetisation occurs due to the relaxation of the protons in the rotating frame with a time constant $T_{1\rho}$. In order to get reasonable ^{13}CO CP MAS spectra, $T_{1\rho}(^1H)$ must be longer than T_{CH}, and T_1 must be short enough to allow effective accumulation of the free induction decay.

In order to assess the above conditions, proton relaxation times T_1 and $T_{1\rho}$ have been measured for $[Ni_6(CO)_{12}]^{2-}$ with four different cations and the results obtained are shown in Table 3. All four compounds have short T_1 values which allow a recycle delay of 2 s to be used. The $T_{1\rho}$ values are long enough to have a contact time, t_m, of 1–2 ms, which is the time used to

Table 2 Minimum H · · · CO contacts for $[Ni_6(CO)_{12}]^{2-}$ with different cations

	d(H · · · CO)/Å	
Cation	Terminal CO	Bridging CO
$[NMe_4]^+$ [5]	3.173	3.160
$[AsPh_4]^+$	2.952	2.853
$[N(PPh_3)_2]^+$ [6]	2.916	3.204

measure ^{13}C signals for hydrocarbons, although the $T_{1\rho}$ values for the $[NMe_4]^+$ and $[N(PPh_3)_2]^+$ salts are one order of magnitude longer than those for the $[NEt_4]^+$ and $[AsPh_4]^+$ salts. Consequently, if T_{CH} is less than 1 ms it should be relatively easy to obtain ^{13}CO CP MAS spectra for all four compounds.

Magnetisation transfer occurs through dipole–dipole interactions between ^{13}C and ^{1}H, and these interactions are proportional to r^{-6} where r denotes the C–H distance. In the case of hydrocarbons, the direct C–H contact r is about 1 Å, and T_{CH} is less than 1 ms. For this intramolecular cross-polarisation it has also been shown that the efficiency of cross-polarisation decreases dramatically with the onset of molecular motion.[12]

In metal carbonyl clusters, however, the distances between the carbons of the CO groups and the hydrogens of the cation are considerably longer than 1 Å (see Table 2). In fact, for $[NMe_4]_2[Ni_6(CO)_{12}]$[5] the shortest interatomic H · · · CO distance is 3.16 Å and, as a result T_{CH} will be longer than 1 ms and becomes comparable with the value of $T_{1\rho}(^1H)$ for the salts of $[Ni_6(CO)_{12}]^{2-}$. These data suggest that it should be difficult to observe ^{13}C CP MAS CO spectra for transition-metal carbonyl clusters, irrespective of molecular motion. However, in spite of these considerations, well resolved spectra are observed when using the $[NMe_4]^+$ cation.

Other factors which have been found to affect the signal-to-noise ratio in CP MAS measurements are line broadening caused by various dynamic effects. Thus, the variation in linewidth can result from (*i*) chemical intraexchange as is often observed in solution, (*ii*) dynamic molecular reorientations which occur with a similar frequency to the radiofrequency decoupling field, and (*iii*) coupling between the MAS rate and chemical shift anisotropy. In the case of (*i*) peak coalescence of the terminal and bridging CO groups may be triggered by slow intraexchange ($\tau_c = 10^{-3}$–10^{-4} s: $\Delta\delta = 40$ ppm); such fluxional processes are often observed in solution NMR studies but not for $[Ni_6(CO)_{12}]^{2-}$. In contrast to the Cotton mechanism[11] for terminal–bridge carbonyl exchange which is well established in solution, there is some evidence for restricted reorientation of the metal skeleton within the carbonyl cage for $[Co_4(CO)_{12}]$[1,2] and $[Fe_2Os(CO)_{12}]$.[14] However, it appears to us unlikely that this reorientation of the metal skeleton within the carbonyl framework can be markedly affected by the variation in packing effects caused by different cations and is an unlikely explanation for the variation in signal-to-noise ratio observed in Fig. 1.

For (*ii*) Rothwell and Waugh[15] have found relationship (3)

$$\frac{1}{T_2} = \frac{\gamma_H^2 \gamma_C^2 \hbar^2}{5r^6}\left(\frac{\tau_c}{1 + \omega_1^2 \tau_c^2}\right) \quad (3)$$

for CP MAS NMR linewidths from temperature-dependent studies, where the protons are subjected to a radiofrequency decoupling of intensity ω_1. According to equation (3) the linewidth becomes a maximum when $\omega_1\tau_c = 1$. This mechanism of line broadening has been clearly observed in the ^{13}CO spectra of $[M(\eta^6\text{-}C_6H_5Me)(CO)_3]$ (M = Cr or Mo)[16] and $[Cr(\eta^6\text{-}C_6H_6)(CO)_3]$.[17] In all cases, the correlation time (τ_c) for the C_3 rotation of the $M(CO)_3$ group satisfies the condition $\omega_1\tau_c = 1$ as a result of τ_C being 10^{-4}–10^{-5} s. This condition also holds at the temperature at which the $T_{1\rho}$ minimum appears.

In the case of $[NMe_4]^+$ it has been shown that both reorientation of the CH_3 group about a C_3 axis and overall reorientation of the whole cation at room temperature occurs in the region of $\omega_1\tau_c \ll 1$ ($\tau_c \ll 10^{-5}$ s, short correlation limit) in many kinds of solids, *e.g.* NMe_4X (X = Cl, Br or I),[18] NMe_4ClO_3[19] and $[NMe_4]_2[MCl_6]$ (M = Pb, Sn or Te).[20] These results are consistent with our $T_{1\rho}$ measurements on $[NMe_4]_2[Ni_6(CO)_{12}]$ and must be one of the reasons why it is possible to observe such intense, sharp carbonyl resonances for $[NMe_4]_2[Ni_6(CO)_{12}]$. It is also worth noting that the rapid isotropic motion of the cation results in a very small chemical shift anisotropy of the methyl carbon so that it is possible to detect the carbonyl resonances separately as shown in Fig. 1(*a*).

When the cation becomes intermediate in size, *e.g.* $[NEt_4]^+$ or

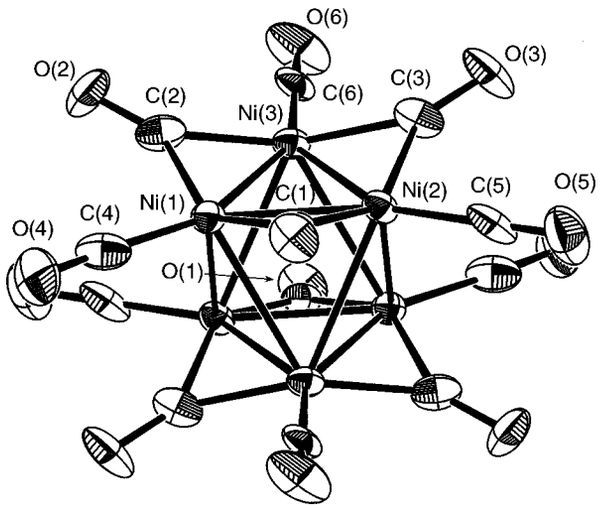

Fig. 5 Molecular structure of the cluster anion of $[AsPh_4]_2[Ni_6(CO)_{12}]$

Table 3 Proton relaxation times T_1 and $T_{1\rho}$ of $A_2[Ni_6(CO)_{12}]$ at room temperature

A	T_1/ms	$T_{1\rho}$/ms
$[NMe_4]^+$	220	124
$[NEt_4]^+$	87	17
$[AsPh_4]^+$	243	12
$[N(PPh_3)_2]^+$	380	216

Table 4 Selected bond lengths (Å) and angles (°) for $[AsPh_4]_2[Ni_6(CO)_{12}]$

Ni(1)–Ni(2)	2.386(2)	Ni(1)–C(4)	1.77(1)
Ni(1)–Ni(2*)	2.847(3)	Ni(2)–C(1)	1.88(1)
Ni(1)–Ni(3)	2.377(2)	Ni(2)–C(3)	1.90(1)
Ni(1)–Ni(3*)	2.749(2)	Ni(2)–C(5)	1.74(1)
Ni(2)–Ni(3)	2.375(2)	Ni(3)–C(2)	1.87(1)
Ni(2)–Ni(3*)	2.740(2)	Ni(3)–C(3)	1.87(1)
Ni(1)–C(1)	1.90(1)	Ni(3)–C(6)	1.76(1)
Ni(1)–C(2)	1.89(1)	C(1) · · · H(16)	2.853
Ni(2)–Ni(1)–Ni(3)	59.84(6)	Ni(3)–Ni(2)–Ni(3*)	87.40(7)
Ni(1)–Ni(2)–Ni(3)	59.90(7)	Ni(1)–Ni(2)–Ni(3*)	64.44(6)
Ni(1)–Ni(3)–Ni(2)	60.26(7)	Ni(2)–Ni(3)–Ni(2*)	92.60(7)
Ni(2)–Ni(1)–Ni(2*)	89.75(7)	Ni(3)–Ni(2)–Ni(1*)	62.75(6)
Ni(2)–Ni(1)–Ni(3*)	64.03(6)	Ni(2)–Ni(3)–Ni(1*)	67.20(7)
Ni(3)–Ni(1)–Ni(3*)	87.15(7)	Ni(1)–Ni(3)–Ni(1*)	92.85(7)
Ni(2*)–Ni(1)–Ni(3*)	62.49(7)	Ni(1)–Ni(3)–Ni(2*)	67.05(7)

$[AsPh_4]^+$, the overall reorientation of the whole cation or the substituents must be slower and then $T_{1\rho}$ approaches a minimum value ($\omega_1\tau_c = 1$). The carbonyl resonances, therefore, start to broaden [see Fig. 2(*b*)] or are completely lost [Fig. 2(*c*)].

For the largest cation, $[N(PPh_3)_2]^+$, we again observe very sharp resonances (Fig. 3). In this case, the molecular motion of the relatively rigid cation is expected to be in the region of $\omega_1\tau_c \gg 1$ ($\tau_c \gg 10^{-3}$ s, long correlation limit) in the solid state. This is consistent with the $T_{1\rho}$ value in Table 2 and from equation (3) a very narrow linewidth is to be expected. The observed linewidth at 333 K is the same as that observed at room temperature, suggesting that the molecular motion is still in the slow limit even at 333 K.

Recently Barrie *et al.*[21] have pointed out that mechanism (*iii*) can cause line broadening in solid $[Cr(\eta^6\text{-}C_6Me_5H)(CO)_3]$ when the rate of chemical exchange becomes comparable with the magnitude of the chemical shift anisotropy ($\Delta\sigma = 32.9$ kHz). For the different salts of $[Ni_6(CO)_{12}]^{2-}$ there is only a very weak MAS rate dependence on the lineshape for the $[N(PPh_3)_2]^+$ salt (see Fig. 3). However, the time-scale ($\tau_c = 10^{-4}$–10^{-5} s) responsible for this mechanism is almost identical to that in case (*ii*). It is, therefore, difficult to distinguish between these two mechanisms.

Finally, another mechanism resulting from high-speed sample spinning can sometimes prolong T_{CH} and reduce the intensity of the ^{13}C CP MAS resonance.[22,23] However, this cannot occur for $A_2[Ni_6(CO)_{12}]$ {A = $[NMe_4]^+$, $[NEt_4]^+$, $[AsPh_4]^+$ or $[N(PPh_3)_2]^+$} because the spectral intensity has negligible spinning-rate dependence between 2.5 and 4 kHz.

In conclusion, ^{13}CO CP MAS spectra with good signal-to-noise ratio (*ca.* 1 : 1) at natural ^{13}CO abundance are observed for carbonyl anions when a small, proton-containing, spherical cation, as exemplified by $[NMe_4]^+$, is used. This must mainly result from the combined effects of very rapid cation motion and the site symmetry of the anion, and should prove useful for the study of other anionic carbonyl clusters.

Experimental

The compound $[NMe_4]_2[Ni_6(CO)_{12}]$ was prepared as described previously[5,7] and salts containing other cations were prepared by metathetical exchange with the appropriate cation. Solid-state NMR measurements were carried out on a Bruker MSL200WB spectrometer using a 7 mm rotor and $T_{1\rho}$ values were obtained using standard procedures from CP MAS measurements.

Crystallography

A dark red crystal of $[AsPh_4]_2[Ni_6(CO)_{12}]$ of dimensions 0.35 × 0.15 × 0.25 mm was mounted on a glass fibre. Using a Rigaku AFC6S diffractometer and Mo-Kα radiation (λ = 0.710 73 Å), cell dimensions were determined from angular settings of 25 reflections with 2θ between 20.48 and 31.57°.

Crystal_data. $C_{60}H_{40}As_2Ni_6O_{12}$, $M = 1455$, triclinic, space group $P\bar{1}$, $a = 11.760(5)$, $b = 12.648(5)$, $c = 11.266(6)$ Å, $\alpha = 103.15(4)$, $\beta = 117.42(3)$, $\gamma = 95.72(4)°$, $U = 1407(1)$ Å^3, $Z = 1$, $D_c = 1.717$ g cm^{-3}, $F(000) = 730$, $\mu = 32.02$ cm^{-1}.

Data collection and processing. Scan mode ω–2θ with ω scan width = (1.37 + 0.30tan θ)°. 4928 Unique reflections recorded ($\theta_{max} = 25°$, $0 \leqslant h \leqslant 12$, $-14 \leqslant k \leqslant 14$, $-13 \leqslant l \leqslant 11$) of which 3128 with $I > 3\sigma(I)$ were used in refinement. Temperature 153 K. Empirical absorption correction based on azimuthal scans applied. Three standard reflections showed no significant variation during data collection.

Structure analysis and refinement. The structure was solved by direct methods using the TEXSAN package.[13] All non-hydrogen atoms were refined anisotropically (based on F^2). The hydrogen atoms were placed in calculated positions and not refined. Final unweighted and weighted agreement factors $\{R = \Sigma(|F_o| - |F_c|)/\Sigma|F_o|$, $R' = [\Sigma w(|F_o| - |F_c|)^2/\Sigma w(F_o)^2]^{\frac{1}{2}}\}$ were 0.054 and 0.067 respectively. A weighting scheme $[w = 1/\sigma^2(F_o)]$ including a factor ($p = 0.03$) to downweight intense reflections was used. The final electron-density difference map showed no peaks >1.27 or <−0.75 e Å^{-3}. Selected bond lengths and angles are given in Table 4 and the structure of $[Ni_6(CO)_{12}]^{2-}$ in Fig. 5.

Atomic coordinates, thermal parameters, and bond lengths and angles have been deposited at the Cambridge Crystallographic Data Centre (CCDC). See Instructions for Authors, *J. Chem. Soc., Dalton Trans.*, 1997, Issue 1. Any request to the CCDC for this material should quote the full literature citation and the reference number 186/343.

Acknowledgements

We thank the Japan Society for the Promotion of Science, the Royal Society, the British Council and the EC (contract No. CHRX-CT93-0277) for financial support. We also thank Mr. J. V. Barkley for help with the X-ray data collection.

References

1 B. T. Heaton, J. Sabounchei, S. Kernaghan, H. Nakayama, T. Eguchi, S. Takeda, N. Nakamura and H. Chihara, *Bull. Chem. Soc. Jpn.*, 1990, **63**, 3019.
2 T. Eguchi, H. Nakayama, H. Ohki, S. Takeda, N. Nakamura, S. Kernaghan and B. T. Heaton, *J. Organomet. Chem.*, 1992, **428**, 207.
3 T. Eguchi, B. T. Heaton, R. Harding, K. Miyagi, G. Longoni, J. Nähring, N. Nakamura, H. Nakayama, T. A. Pakkanen, J. Pursiainen and A. K. Smith, *J. Chem. Soc., Dalton Trans.*, 1996, 625.
4 T. Eguchi, R. Harding, B. T. Heaton, G. Longoni, K. Miyagi, J. Nahring, N. Nakamura, H. Nakayama and A. K. Smith, unpublished work.
5 J. C. Calabrese, L. F. Dahl, P. Chini, G. Longoni and S. Martinengo, *J. Am. Chem. Soc.*, 1974, **96**, 2616.
6 R. E. Bachmann and K. H. Whitmire, *Acta Crystallogr.*, 1993, **49**, 1121.
7 G. Longoni, B. T. Heaton and P. Chini, *J. Chem. Soc., Dalton Trans.*, 1980, 1537.
8 E. O. Stejskal, J. Schaefer and T. R. Steger, *Faraday Symp. Chem. Soc.*, 1979, **13**, 56.
9 M. Mehring, *Principals of High Resolution NMR in Solids*, Springer, Berlin, 1983.
10 R. Voelkel, *Angew. Chem., Int. Ed. Engl.*, 1988, **27**, 1468.
11 F. A. Cotton and B. E. Hanson, *Rearrangements in Ground and Excited States*, ed. P. de Mayo, Academic Press, New York, 1980, p. 379.
12 D. Schulze, H. Ernst, D. Fenzke, W. Meiler and H. Pfeifer, *J. Phys. Chem.*, 1990, **94**, 3499.
13 TEXSAN-TEXRAY, Structure Analysis Package, Molecular Structure Corporation, Houston, TX, 1985.
14 D. Braga, L. J. Farrugia, F. Grepioni and A. Senior, *J. Chem. Soc., Chem. Commun.*, 1995, 1219; L. J. Farrugia, A. M. Senior, D. Braga, F. Grepioni, A. G. Orpen and J. G. Crossley, *J. Chem. Soc., Dalton Trans.*, 1996, 631.
15 W. P. Rothwell and J. S. Waugh, *J. Chem. Phys.*, 1981, **74**, 2721.
16 G. W. Wagner and B. E. Hanson, *Inorg. Chem.*, 1987, **26**, 2019.
17 A. E. Aliev, K. D. M. Harris, F. Guillaume and P. J. Barrie, *J. Chem. Soc., Dalton Trans.*, 1994, 3193.
18 S. Albert, H. S. Gutowsky and J. A. Ripmeester, *J. Chem. Phys.*, 1972, **56**, 3672.
19 T. Tsuneyoshi, N. Nakamura and H. Chihara, *J. Magn. Reson.*, 1977, **27**, 191.
20 Y. Furukawa, Y. Baba, S. Gima, M. Kaga, T. Asaji, R. Ikeda and D. Nakamura, *Z. Naturforsch., Teil A*, 1991, **46**, 809.
21 P. J. Barrie, C. A. Mitsopoulou and E. W. Randall, *J. Chem. Soc., Dalton Trans.*, 1995, 2125.
22 J. R. Long, B. Q. Sun, A. Bowen and R. G. Griffin, *J. Am. Chem. Soc.*, 1994, **116**, 11950.
23 S. Hedinger, B. H. Meier and R. R. Ernst, *J. Chem. Phys.*, 1995, **102**, 4000.

Received 10*th June* 1996; *Paper* 6/04078K